ISSN 1674-1056
http://cpb.iphy.ac.cn
http://iopscience.iop.org/cpb
中国物理 B
Chinese Physics
中国物理
Chinese Physics B

Implementation of quantum phase gate between two atoms via Rydberg antiblockade and adiabatic passage

Xi Tan(谭曦), Jin-Lei Wu(吴金雷), Can Deng(邓灿), Wei-Jian Mao(毛伟建), Hai-Tao Wang(王海涛), Xin Ji(计新)

Citation: Chin. Phys. B . 2018, 27(10): 100307. **doi:** 10.1088/1674-1056/27/10/100307

Journal homepage: http://cpb.iphy.ac.cn; http://iopscience.iop.org/cpb

What follows is a list of articles you may be interested in

Thermal quantum correlations of a spin-1/2 Ising-Heisenberg diamond chain with Dzyaloshinskii-Moriya interaction

Yidan Zheng(郑一丹), Zhu Mao(毛竹), Bin Zhou(周斌)

Chin. Phys. B . 2018, 27(9): 090306. **doi:** 10.1088/1674-1056/27/9/090306

Invariants-based shortcuts for fast generating Greenberger—Horne—Zeilinger state among three superconducting qubits

Jing Xu(徐晶), Lin Yu(于琳), Jin-Lei Wu(吴金雷), Xin Ji(计新)

Chin. Phys. B . 2017, 26(9): 090301. **doi:** 10.1088/1674-1056/26/9/090301

Conditions on converting coherence into entanglement

Lian-Wu Yang(杨连武), Yun-Jie Xia(夏云杰)

Chin. Phys. B . 2017, 26(8): 080302. **doi:** 10.1088/1674-1056/26/8/080302

Production and detection of ultracold Cs_2 molecules via four-photon adiabatic passage

Li Jian, Liu Yong, Cong Shu-Lin

Chin. Phys. B . 2014, 23(1): 010308. **doi:** 10.1088/1674-1056/23/1/010308

Generation of four-atom Greenberger-Horn-Zeilinger state via adiabatic passage

Zhang Chun-Ling, Chen Mei-Feng

Chin. Phys. B . 2013, 22(5): 050307. **doi:** 10.1088/1674-1056/22/5/050307

Implementation of quantum phase gate between two atoms via Rydberg antiblockade and adiabatic passage*

Xi Tan(谭曦), Jin-Lei Wu(吴金雷), Can Deng(邓灿),
Wei-Jian Mao(毛伟建), Hai-Tao Wang(王海涛), and Xin Ji(计新)†

Department of Physics, College of Science, Yanbian University, Yanji 133002, *China*

(Received 1 June 2018; revised manuscript received 17 July 2018; published online 10 September 2018)

Combining adiabatic passage and Rydberg antiblockade, we propose a scheme to implement a two-qubit phase gate between two Rydberg atoms. Detuning parameters between frequencies of atomic transitions and those of the corresponding driving lasers are carefully chosen to offset the blockade effect of two Rydberg atoms, so that an effective Hamiltonian, representing a single-photon detuning Λ-type three-level system and concluding the quantum state of two Rydberg atoms excited simultaneously, is obtained. The adiabatic-passage technique, based on the effective Hamiltonian, is adopted to implement a two-atom phase gate by using two time-dependent Rabi frequencies. Numerical simulations indicate that a high-fidelity two-qubit π-phase gate is constructed and its operation time does not have to be controlled accurately. Besides, owing to the long coherence time of the Rydberg state, the phase gate is robust against atomic spontaneous emission.

Keywords: quantum phase gate, Rydberg antiblockade, adiabatic passage

PACS: 03.67.Bg, 42.50.Dv, 42.50.Ex **DOI:** 10.1088/1674-1056/27/10/100307

1. Introduction

Compared with a classical computer, a quantum computer possesses greater capability and faster speed to solve some enormous problems and process massive amounts of information; therefore, it has attracted attention from researchers in recent decades.[1–3] As is well known, all gate operations in quantum computation can be constructed by a series of elementary one-qubit unitary gates and two-qubit logical gates.[4,5] To put quantum computing into practice, therefore, the quantum gate has been studied theoretically and experimentally in the past several decades.[6–15] A lot of schemes of implementing quantum gates have been proposed by using diverse physical systems, such as the ion-trap system,[16] linear optical system,[17] cavity-QED system,[18–20] NMR system,[21] and superconducting system.[22,23]

As a promising candidate for implementing quantum computation, neutral atoms are of particular interest because of the long coherence time of internal atomic states. Their stable hyperfine energy states are especially suited for encoding logic qubits, and are easily controllable and measurable by using a resonant laser pulse.[24] On the other hand, neutral atoms exhibit large dipole moments when they are excited to Rydberg states, which induces powerful and long-range van der Waals or dipole–dipole interaction. This interaction between the excited Rydberg atoms can lead to Rydberg blockade suppressing resonant optical excitation of over-one Rydberg atoms.[25,26] Many protocols of quantum information processing have been proposed via Rydberg–Rydberg interaction (RRI).[27–33] Instead, when a certain relation between Rydberg interaction strength and the detuning between frequencies of atomic transitions and those of corresponding driving lasers is satisfied, the atoms can also be collectively excited to Rydberg states, which results in the so-called Rydberg antiblockade. In the last several years, the Rydberg antiblockade mechanism has been widely applied in quantum information processing and quantum computation.[34–43] For example, Su *et al.* implemented quantum gates in the presence of Rydberg antiblockade;[36–38] Shao *et al.* came up with the Rydberg ground-state antiblockade regime;[39,40] and then Ji *et al.*[41] and Zhao *et al.*[42] proposed schemes to fuse entanglement and generate entanglement, respectively, via Rydberg ground-state antiblockade.

In this paper, we propose a scheme for the implementation of a quantum phase gate between two atoms by combining adiabatic passage and Rydberg antiblockade. We carefully design the detuning between frequencies of atomic transitions and those of corresponding driving lasers so as to compensate the blockade effect of two Rydberg atoms. An effective Hamiltonian, which denotes a single-photon detuning Λ-type three-level system and involves the quantum state of two atoms excited simultaneously, is obtained. In the context of the Λ-type three-level effective Hamiltonian, the adiabatic-passage technique is employed to implement a two-qubit phase gate by adopting two time-dependent Rabi frequencies. Adiabatic passage is widely used by slowly varying time-dependent parameters to drive the evolution of a quantum system along its certain eigenstate, generally a dark state with zero eigenenergy, to achieve the desired population transfer. The successful

*Project supported by the National Natural Science Foundation of China (Grant No. 11464046).
†Corresponding author. E-mail: jixin@ybu.edu.cn
© 2018 Chinese Physical Society and IOP Publishing Ltd

implementation of the two-qubit phase gate by means of adiabatic passage means that the access to the high-fidelity phase gate does not require the precise control of operation time, and that the scheme is robust against atomic spontaneous emission with a very low Rydberg-state dissipative rate.

2. Model and effective dynamics

Figure 1 shows the physical model for implementing the two-qubit phase gate. There are two Rydberg atoms trapped in two separated microscopic dipole traps. Atom 1 possesses one high-lying Rydberg state $|r\rangle$ and two hyperfine ground states $|0\rangle$ and $|1\rangle$, while atom 2 has one more ground state $|g\rangle$ than atom 1. For atom 1, transitions $|1\rangle_1 \leftrightarrow |r\rangle_1$ and $|0\rangle_1 \leftrightarrow |r\rangle_1$ are driven by classical lasers with Rabi frequencies Ω_1 and Ω_2' and corresponding red detuning Δ_1 and blue detuning Δ_2, respectively. For atom 2, transitions $|1\rangle_1 \leftrightarrow |r\rangle_1$ and $|g\rangle_1 \leftrightarrow |r\rangle_1$ are driven by classical lasers with Rabi frequencies Ω_1' and Ω_2 and corresponding blue detuning Δ_2 and red detuning Δ_1, respectively. The quantum information is coded in quantum states $|0\rangle$ and $|1\rangle$ of two atoms, and the desired transformation for the target π-phase gate is

$$\begin{aligned} &|00\rangle \to |00\rangle, \quad |01\rangle \to |01\rangle, \\ &|10\rangle \to |10\rangle, \quad |11\rangle \to -|11\rangle. \end{aligned} \tag{1}$$

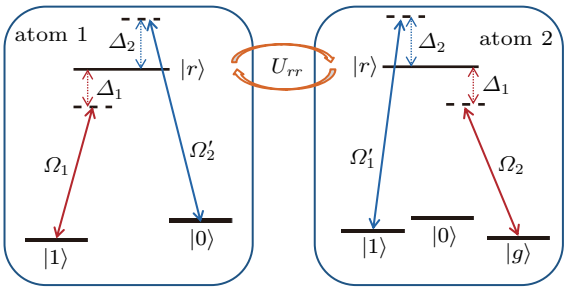


Fig. 1. (color online) Sketch of atomic level structures and transitions.

With rotating-wave approximation, the Hamiltonian of the whole system can be written as (assuming $\hbar = 1$):

$$\begin{aligned} H_0 \;=\; & (\Omega_1|r\rangle_1\langle 1| + \Omega_2'|r\rangle_1\langle 0| \\ & + \Omega_1'|r\rangle_2\langle 1| + \Omega_2|r\rangle_2\langle g| + \text{H.c.}) \\ & - \Delta_1(|1\rangle_1\langle 1| + |g\rangle_2\langle g|) \\ & + \Delta_2(|0\rangle_1\langle 0| + |1\rangle_2\langle 1|) + U_{rr}|rr\rangle\langle rr|, \end{aligned} \tag{2}$$

with U_{rr} being RRI strength dependent on the principal quantum numbers of Rydberg states and the distance between the Rydberg atoms. The evolution of the whole system is governed by Schrödinger equation $\mathrm{i}\partial|\Psi(t)\rangle/\partial t = H_0|\Psi(t)\rangle$, in which the state of the whole system at an arbitrary time can be written as the time-dependent superposition of the direct product states of two atoms

$$\begin{aligned} |\Psi(t)\rangle \;=\; & C_{00}|00\rangle + C_{01}|01\rangle + C_{0g}|0g\rangle + C_{0r}|0r\rangle \\ & + C_{10}|10\rangle + C_{11}|11\rangle + C_{1g}|1g\rangle + C_{1r}|1r\rangle \\ & + C_{r0}|r0\rangle + C_{r1}|r1\rangle + C_{rg}|rg\rangle + C_{rr}|rr\rangle, \end{aligned} \tag{3}$$

in which, for convenience, the time-dependence label "(t)" of the probability amplitude $C_{mn}(t)$ ($m = 0, 1, r$; $n = 0, 1, g, r$) is dropped. With the direct product states $\{|mn\rangle\}$ being basis vectors and moving H_0 in Eq. (2) to a rotation frame with respect to $\exp(-\mathrm{i}H_0't)$, for which $H_0' = -\Delta_1(|1\rangle_1\langle 1| + |g\rangle_2\langle g|) + \Delta_2(|0\rangle_1\langle 0| + |1\rangle_2\langle 1|) + U_{rr}|rr\rangle\langle rr|$, we have

$$\begin{aligned} H_1 \;=\; & \Omega_1\,\mathrm{e}^{\mathrm{i}\Delta_1 t}(|r0\rangle\langle 10| + |r1\rangle\langle 11| + |rg\rangle\langle 1g| + \mathrm{e}^{\mathrm{i}U_{rr}t}|rr\rangle\langle 1r|) \\ & + \Omega_2'\,\mathrm{e}^{-\mathrm{i}\Delta_2 t}(|r0\rangle\langle 00| + |r1\rangle\langle 01| \\ & + |rg\rangle\langle 0g| + \mathrm{e}^{\mathrm{i}U_{rr}t}|rr\rangle\langle 0r|) \\ & + \Omega_1'\,\mathrm{e}^{-\mathrm{i}\Delta_2 t}(|0r\rangle\langle 01| + |1r\rangle\langle 11| + \mathrm{e}^{\mathrm{i}U_{rr}t}|rr\rangle\langle r1|) \\ & + \Omega_2\,\mathrm{e}^{\mathrm{i}\Delta_1 t}(|0r\rangle\langle 0g| + |1r\rangle\langle 1g| \\ & + \mathrm{e}^{\mathrm{i}U_{rr}t}|rr\rangle\langle rg|) + \text{H.c.} \end{aligned} \tag{4}$$

By imposing the relation $U_{rr} = \Delta_2 - \Delta_1$ and the large-detuning condition $\Delta_{1,2} \gg \Omega_1, \Omega_1', \Omega_2, \Omega_2'$, an effective Hamiltonian is induced as[44]

$$\begin{aligned} H_1' \;=\; & \delta_{00}|00\rangle\langle 00| + \delta_{01}|01\rangle\langle 01| + \delta_{10}|10\rangle\langle 10| \\ & + \delta_{11}|11\rangle\langle 11| + \delta_{0g}|0g\rangle\langle 0g| + \delta_{rr}|rr\rangle\langle rr| \\ & + \delta_{r0}|r0\rangle\langle r0| + \delta_{r1}|r1\rangle\langle r1| + \delta_{1g}|1g\rangle\langle 1g| \\ & + \delta_{1r}|1r\rangle\langle 1r| + \delta_{rg}|rg\rangle\langle rg| + \delta_{0r}|0r\rangle\langle 0r| \\ & + (\Omega_\mathrm{a}|rr\rangle\langle 11| + \Omega_\mathrm{b}|rr\rangle\langle 0g| \\ & + \Omega_\mathrm{a}'|rg\rangle\langle 1r| + \Omega_\mathrm{b}'|0r\rangle\langle r1| + \text{H.c.}), \end{aligned} \tag{5}$$

with

$$\begin{aligned} &\delta_{00} = \frac{\Omega_2'^2}{\Delta_2}, \quad \delta_{01} = \frac{\Omega_2'^2}{\Delta_2} + \frac{\Omega_1'^2}{\Delta_2}, \quad \delta_{10} = -\frac{\Omega_1^2}{\Delta_1}, \\ &\delta_{11} = \frac{\Omega_1'^2}{\Delta_2} - \frac{\Omega_1^2}{\Delta_1}, \quad \delta_{0g} = \frac{\Omega_2'^2}{\Delta_2} - \frac{\Omega_2^2}{\Delta_1}, \\ &\delta_{rr} = \frac{\Omega_1^2}{\Delta_2} + \frac{\Omega_2^2}{\Delta_2} - \frac{\Omega_1'^2}{\Delta_1} - \frac{\Omega_2'^2}{\Delta_1} - \frac{\Omega_1\Omega_2'}{\Delta_1}, \\ &\delta_{r0} = \frac{\Omega_1^2}{\Delta_1} - \frac{\Omega_2'^2}{\Delta_2}, \quad \delta_{r1} = \frac{\Omega_1^2 + \Omega_1'^2}{\Delta_1} - \frac{\Omega_2'^2}{\Delta_2}, \\ &\delta_{1g} = -\frac{\Omega_1^2 + \Omega_2^2}{\Delta_1}, \quad \delta_{1r} = \frac{\Omega_2^2}{\Delta_1} - \frac{\Omega_1^2 + \Omega_1'^2}{\Delta_2}, \\ &\delta_{rg} = \frac{\Omega_1^2}{\Delta_1} - \frac{\Omega_2^2 + \Omega_2'^2}{\Delta_2}, \quad \delta_{0r} = \frac{\Omega_2^2 + \Omega_2'^2 + \Omega_1'\Omega_2'}{\Delta_1} - \frac{\Omega_1'^2}{\Delta_2}, \\ &\Omega_\mathrm{a} = \frac{\Omega_1\Omega_1'}{\Delta_2} - \frac{\Omega_1\Omega_1'}{\Delta_1}, \quad \Omega_\mathrm{b} = \frac{\Omega_2\Omega_2'}{\Delta_2} - \frac{\Omega_2\Omega_2'}{\Delta_1}, \\ &\Omega_\mathrm{a}' = \frac{\Omega_1\Omega_2}{\Delta_1} - \frac{\Omega_1\Omega_2}{\Delta_2}, \quad \Omega_\mathrm{b}' = \frac{\Omega_1'\Omega_2'}{\Delta_1} - \frac{\Omega_1'\Omega_2'}{\Delta_2}, \end{aligned}$$

in which δ_k ($k = 00$, 01, 10, 11, $0g$, rr, $r0$, $r1$, $1g$, $1r$, rg, $0r$) originates from the Stark shift of the quantum state $|k\rangle$. $\Omega_{\mathrm{a(b)}}$, Ω_a', and Ω_b' are effective coupling strengths between $|rr\rangle$ and $|11\rangle$ ($|0g\rangle$), $|rg\rangle$ and $|1r\rangle$, and $|0r\rangle$ and $|r1\rangle$, respectively. By ignoring the terms decoupled to $\{|00\rangle, |01\rangle, |10\rangle, |11\rangle\}$, the effective Hamiltonian H_1' becomes

$$H_2 \;=\; \delta_{00}|00\rangle\langle 00| + \delta_{01}|01\rangle\langle 01| + \delta_{10}|10\rangle\langle 10|$$

$$+\delta_{11}|11\rangle\langle 11|+\delta_{0g}|0g\rangle\langle 0g|+\delta_{rr}|rr\rangle\langle rr| +(\Omega_{\rm a}|rr\rangle\langle 11|+\Omega_{\rm b}|rr\rangle\langle 0g|+{\rm H.c.}). \quad (6)$$

Then by introducing auxiliary levels and appropriate transitions,[42] the terms of ground-state Stark shifts can be eliminated, and thus the Hamiltonian H_2 in Eq. (6) becomes

$$H_{\rm eff} = \delta_{rr}|rr\rangle\langle rr|+(\Omega_{\rm a}|rr\rangle\langle 11|+\Omega_{\rm b}|rr\rangle\langle 0g|+{\rm H.c.}), \quad (7)$$

which is a Hamiltonian of the single-photon detuning Λ-type three-level system. Besides, Hamiltonian $H_{\rm eff}$ involves the quantum state $|rr\rangle$ of two-atom simultaneous excitation, which is caused by the Rydberg-antiblockade effect. Governed by $H_{\rm eff}$, the state of the effective system at an arbitrary time can be written as

$$|\Psi^{\rm e}(t)\rangle = C^{\rm e}_{11}(t)|11\rangle+C^{\rm e}_{0g}(t)|0g\rangle+C^{\rm e}_{rr}(t)|rr\rangle. \quad (8)$$

3. Implementing two-qubit π-phase gate via adiabatic passage

Hamiltonian $H_{\rm eff}$ in Eq. (7) does not involve $|00\rangle$, $|01\rangle$, and $|10\rangle$, which indicates that $|00\rangle\rightarrow|00\rangle$, $|01\rangle\rightarrow|01\rangle$, and $|10\rangle\rightarrow|10\rangle$ are accessible readily. If $|11\rangle\rightarrow-|11\rangle$ is accomplished, the target two-qubit π-phase gate will be implemented. In this section, we next show how to achieve $|11\rangle\rightarrow-|11\rangle$ by using adiabatic passage.

First of all, we change Ω_1 and Ω_2 to time-dependent $\Omega_1(t)$ and $\Omega_2(t)$, respectively, while other parameters keep time-independent. Hence, $\Omega_{\rm a}$, $\Omega_{\rm b}$, and δ_{rr} become time-dependent $\Omega_{\rm a}(t)$, $\Omega_{\rm b}(t)$, and $\delta_{rr}(t)$, respectively. The instantaneous eigenstates of Hamiltonian $H_{\rm eff}$ in Eq. (7) are given by

$$\begin{aligned}
|\Phi_+(t)\rangle &= \sin\theta(t)\sin\phi(t)|11\rangle \\
&\quad +\cos\phi(t)|rr\rangle+\cos\theta(t)\sin\phi|0g\rangle, \\
|\Phi_0(t)\rangle &= \cos\theta(t)|11\rangle-\sin\theta(t)|0g\rangle, \\
|\Phi_-(t)\rangle &= \sin\theta(t)\cos\phi(t)|11\rangle \\
&\quad -\sin\phi(t)|rr\rangle+\cos\theta(t)\cos\phi|0g\rangle,
\end{aligned} \quad (9)$$

with corresponding eigenvalues being $\lambda_+(t)=\Omega(t)\cot\phi(t)$, $\lambda_0(t)=0$, and $\lambda_-=-\Omega(t)\tan\phi(t)$, respectively, for which we have defined

$$\Omega(t)=\sqrt{\Omega_{\rm a}(t)^2+\Omega_{\rm b}(t)^2},$$
$$\tan\theta(t)=\frac{\Omega_{\rm a}(t)}{\Omega_{\rm b}(t)},\quad \tan 2\phi(t)=\frac{2\Omega(t)}{\delta_{rr}(t)}. \quad (10)$$

Based on the theory of adiabatic approximation,[45] slowly varying parameters of the quantum system will constrain the transitions between different eigenstates.[46] If the effective system is in an eigenstate $|\Phi_n(t)\rangle$ $(n=+,0,-)$ initially, then at an arbitrary time the state of the effective system will be[47]

$$|\Psi^{\rm e}(t)\rangle = {\rm e}^{{\rm i}[a_n(t)+\gamma_n(t)]}|\Phi_n(t)\rangle, \quad (11)$$

where $a_n(t)=-\int_0^t\lambda_n(t')\,{\rm d}t'$ is the dynamic phase and $\gamma_n(t)={\rm i}\int_0^t\langle\Phi_n(t')|\partial\Phi_n(t')/\partial t'\rangle\,{\rm d}t'$ is the geometric phase. For initial state $|11\rangle$, by setting $\theta(0)=0$ (assuming the evolution starts at $t=0$ and ends at $t=t_{\rm f}$), the effective system is in $|\Phi_0(t)\rangle$ initially. It is easy to know that the dynamic phase and geometric phase are both zero, and at an arbitrary time, hence, the state of the effective system is always $|\Phi_0(t)\rangle$. Therefore, $\theta(0)=0$ and $\theta(t_{\rm f})=\pi$ are expected to accomplish the transformation $|11\rangle\rightarrow-|11\rangle$ (i.e., the target π-phase gate) by following $|\Phi_0(t)\rangle$.

4. Numerical simulations and discussion

In order to meet the boundary conditions $\theta(0)=0$ and $\theta(t_{\rm f})=\pi$, the Rabi frequencies $\Omega_1(t)$ and $\Omega_2(t)$ can be chosen as

$$\begin{aligned}
\Omega_1(t) &= \Omega_0\exp[-((t-t_{\rm c}/2-\tau)/T)^2], \\
\Omega_2(t) &= \Omega_0\exp[-((t-t_{\rm c}/2+\tau)/T)^2] \\
&\quad -\Omega_0\exp[-((t-t_{\rm c}/2-2\tau)/T)^2],
\end{aligned} \quad (12)$$

in which: $T=0.18t_{\rm c}$ is the pulse width; $\tau=0.12t_{\rm c}$ is the pulse delay; and $t_{\rm c}=3000/\Omega_0$ is the long pulse time executed to meet the adiabatic approximation. Correspondingly, the effective Rabi frequencies $\Omega_{\rm a}(t)$ and $\Omega_{\rm a}(t)$ in Eqs. (6) and (7) then can be determined, for which we have chosen other parameters as $\Omega_1'=\Omega_2'=\Omega_0$, $\Delta_1=50\Omega_0$, and $\Delta_2=10\Omega_0$. With these parameters, we plot the time-dependence of $\Omega_{1,2}(t)$ and $\Omega_{\rm a,b}(t)$, respectively, in Figs. 2(a) and 2(b). In addition, in Fig. 2(c) we plot the time dependence of $\theta(t)=\arccos[\Omega_{\rm b}(t)/\Omega(t)]$. Obviously, figure 2 (especially Fig. 2(c)) shows that the boundary conditions $\theta(0)=0$ and $\theta(t_{\rm f})=\pi$ are satisfied very well.

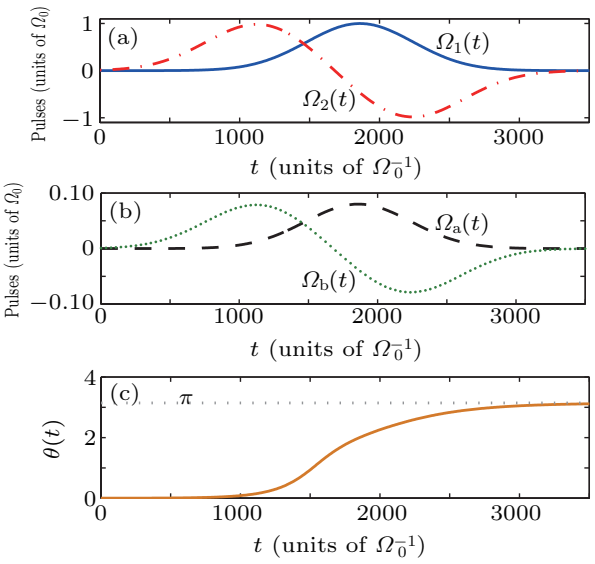


Fig. 2. (color online) (a) Time-dependence of $\Omega_1(t)$ and $\Omega_2(t)$. (b) Time-dependence of $\Omega_{\rm a}(t)$ and $\Omega_{\rm b}(t)$. (c) Time-dependence of $\theta(t)=\arccos[\Omega_{\rm b}(t)/\Omega(t)]$. Parameters used here: $t_{\rm c}=3000/\Omega_0$, $T=0.18t_{\rm c}$, $\tau=0.12t_{\rm c}$, $\Omega_1'=\Omega_2'=\Omega_0$, $\Delta_1=50\Omega_0$, and $\Delta_2=10\Omega_0$.

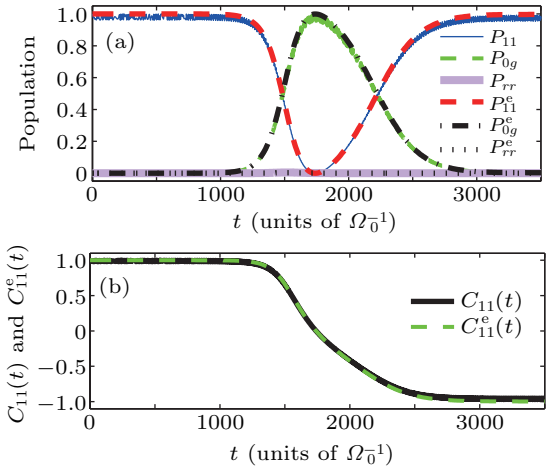


Fig. 3. (color online) (a) Comparison between the population transfer governed by the total Hamiltonian H_0 in Eq. (2) and that governed by the effective Hamiltonian H_{eff} in Eq. (6). (b) Comparison between the variation of $C_{11}(t)$ governed by H_0 and that of $C^{\text{e}}_{11}(t)$ governed by the H_{eff}. Parameters used here are the same as in Fig. 2.

The transformation $|11\rangle \rightarrow -|11\rangle$ is a key to the implementation of the π-phase gate, and in Fig. 3(a), thus with $|11\rangle$ being the initial state, we give a comparison between the population transfer governed by the total Hamiltonian H_0 in Eq. (2) and that governed by the effective Hamiltonian H_{eff} in Eq. (7), for which we have defined $P_k = |C_k(t)|^2$ ($k = 11, rr, 0g$) and $P^{\text{e}}_k = |C^{\text{e}}_k(t)|^2$. More concretely, in Fig. 3(b), we plot the comparison between the variation of $C_{11}(t)$ governed by H_0 and that of $C^{\text{e}}_{11}(t)$ governed by the H_{eff}. Figure 3(a) assisted by Fig. 3(b) proves that the evolution governed by Hamiltonian H_{eff} gives the perfect population transfer of implementing the ideal transformation $|11\rangle \rightarrow -|11\rangle$. Apparently, all curves in Fig. 3 originating from H_0, up to slight oscillations, coincide well with those originating from H_{eff}, which declares that the approximation from H_0 to H_{eff} is effective and predicts that the implementation of the two-qubit π-phase gate with H_0 would be successful.

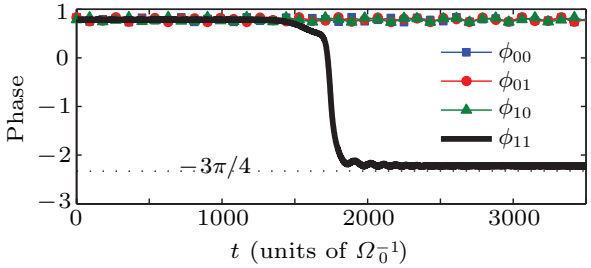


Fig. 4. (color online) Time-dependence of phases for the four different initial states with a complex phase $e^{i\pi/4}$.

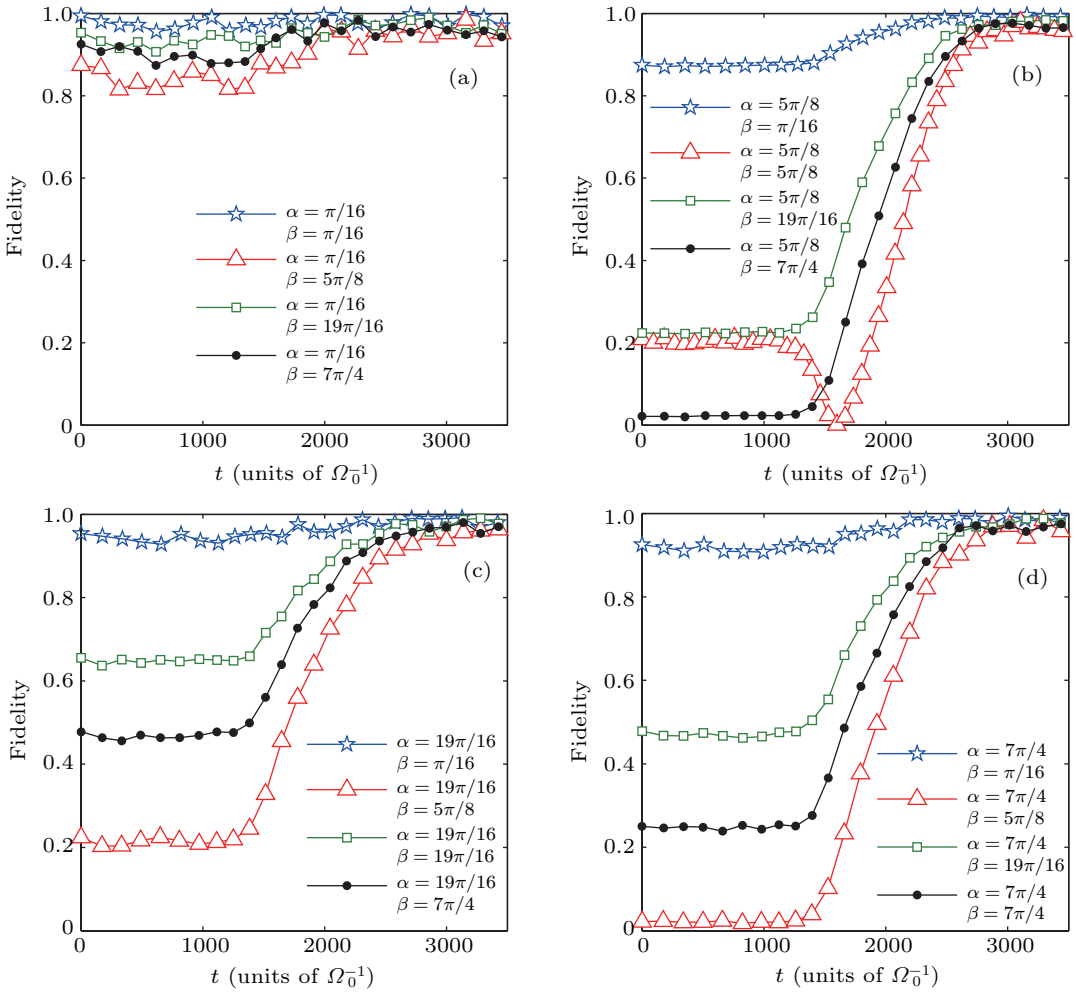


Fig. 5. (color online) Fidelity $F(t) = |\langle\Psi_{\text{ideal}}|\Psi(t)\rangle|^2$ with different pairs of α and β. Parameters used here are the same as in Fig. 2.

For a phase gate, the evolution of the phase of a state is a crucial investigated aspect. Therefore, we explore the evolution of the phase for the four different initial states with a complex phase $e^{i\phi_0}$. For the scheme proposed for a π-phase gate, we desire that if the initial state is $e^{i\phi_0}|00\rangle$, $e^{i\phi_0}|01\rangle$, or $e^{i\phi_0}|10\rangle$, neither the state nor the phase will change at all. For the initial state $e^{i\phi_0}|11\rangle$, however, after adiabatic passage, the state will keep unchanged but the phase will change with π. In Fig. 4, we give the time-dependence of the phase for the initial state $e^{i\phi_0}|M\rangle$ ($M = 00, 01, 10, 11$) whose evolution is dominated by Hamiltonian Eq. (2), for which we have chosen $\phi_0 = \pi/4$ for simplicity. We extract the phase of the state $|M\rangle$ by $\phi_M = -i\ln(C_M/|C_M|)$.[48] As shown in Fig. 4, ϕ_{00}, ϕ_{01}, and ϕ_{10} keep roughly unchanged, i.e., $\pi/4$, except slight fluctuations, while ϕ_{11} is reduced by π with an acceptable approximation after the adiabatic-passage operation, which fits well with expectations. In a word, figure 4 proves that a complex phase involved in the initial state has no influence on the performance of the scheme.

We consider a random initial state read as

$$\begin{aligned}|\Psi_0\rangle &= \cos\alpha\cos\beta|00\rangle + \cos\alpha\sin\beta|01\rangle \\ &\quad + \sin\alpha\cos\beta|10\rangle + \sin\alpha\sin\beta|11\rangle, \end{aligned} \tag{13}$$

and after a π-phase gate operation on $|\Psi_0\rangle$, the outcome state is

$$\begin{aligned}|\Psi_{\text{ideal}}\rangle &= \cos\alpha\cos\beta|00\rangle + \cos\alpha\sin\beta|01\rangle \\ &\quad + \sin\alpha\cos\beta|10\rangle - \sin\alpha\sin\beta|11\rangle. \end{aligned} \tag{14}$$

In Fig. 5, we plot the fidelity $F(t) = |\langle\Psi_{\text{ideal}}|\Psi(t)\rangle|^2$ by picking some pairs of α and β from $\alpha, \beta \in 0 \sim 2\pi$ to test the effectiveness of our scheme with Hamiltonian H_0 for implementing the two-qubit π-phase gate. Further more, in Table 1 we list the final fidelity $F(t_f = 3500\Omega^{-1})$ with different values of α and β, and all final fidelities in Table 1 are over 0.95. All curves in Fig. 5 and data in Table 1 indicate that the scheme with Hamiltonian H_0 for implementing the two-qubit π-phase gate is quite effective.

Table 1. Samples of the final fidelity $F(t_f)$ with different values of α and β.

α	β	$F(t_f)$	α	β	$F(t_f)$
$\pi/16$	$\pi/16$	0.9703	$\pi/16$	$5\pi/8$	0.9516
$\pi/16$	$19\pi/16$	0.9507	$\pi/16$	$7\pi/4$	0.9429
$5\pi/8$	$\pi/16$	0.9923	$5\pi/8$	$5\pi/8$	0.9569
$5\pi/8$	$19\pi/16$	0.9818	$5\pi/8$	$7\pi/4$	0.9651
$19\pi/16$	$\pi/16$	0.9801	$19\pi/16$	$5\pi/8$	0.9634
$19\pi/16$	$19\pi/16$	0.9779	$19\pi/16$	$7\pi/4$	0.9702
$7\pi/4$	$\pi/16$	0.9892	$7\pi/4$	$5\pi/8$	0.9572
$7\pi/4$	$19\pi/16$	0.9768	$7\pi/4$	$7\pi/4$	0.9746

In fact, a sufficient standard of judging the successful implementation of a quantum gate is the average fidelity defined by

$$\bar{F}(t) = \frac{1}{4\pi^2}\int_0^{2\pi}\int_0^{2\pi}\langle\Psi_{\text{ideal}}|\rho(t)|\Psi_{\text{ideal}}\rangle\,\mathrm{d}\alpha\,\mathrm{d}\beta, \tag{15}$$

where $\rho(t)$ is the density operator of the quantum system. In the following, therefore, we take atomic spontaneous emission into account, and then consider the average fidelity of implementing the two-qubit π-phase gate by numerically solving the master equation

$$\begin{aligned}\frac{\partial\rho(t)}{\partial t} &= -i[H_0, \rho(t)] - \frac{1}{2}\sum_{m=1}^{5}[\mathcal{L}_m^\dagger\mathcal{L}_m\rho(t) \\ &\quad - 2\mathcal{L}_m\rho(t)\mathcal{L}_m^\dagger + \rho(t)\mathcal{L}_m^\dagger\mathcal{L}_m], \end{aligned} \tag{16}$$

where $\mathcal{L}_1 = \sqrt{\gamma/2}|0\rangle_1\langle r|$, $\mathcal{L}_2 = \sqrt{\gamma/2}|1\rangle_1\langle r|$, $\mathcal{L}_3 = \sqrt{\gamma/3}|0\rangle_2\langle r|$, $\mathcal{L}_4 = \sqrt{\gamma/3}|1\rangle_2\langle r|$, and $\mathcal{L}_5 = \sqrt{\gamma/3}|g\rangle_2\langle r|$ are Lindblad operators describing the dissipative processes, and γ is the atomic total spontaneous emission rate. In Fig. 6, we plot the time-dependent variation of the average fidelity with different atomic total spontaneous emission rates. As shown in Fig. 6, the greater the atomic total spontaneous emission rate is, the more the final average fidelity descends. Nevertheless, the descent of the final average fidelity is not significant, and even when $\gamma = 0.01\Omega_0$ the final average fidelity is near 0.95. Therefore, we deem that the scheme of implementing the two-qubit π-phase gate is robust against atomic spontaneous emission. After all, the spontaneous emission of Rydberg atoms is far below $0.01\Omega_0$ in practice. In the experiment, the model we proposed to implement the two-qubit π-phase gate can be realized by two ^{87}Rb atoms trapped in two tightly-focused dipole traps.[49,50] Based on the related experimental parameters $\Omega_0 = 2\pi\times 6.8$ MHz and $\gamma = 2\pi\times 4.8$ kHz$\sim 10^{-3}\Omega_0$, the average fidelity of implementing the two-qubit π-phase gate can reach 98.7%.

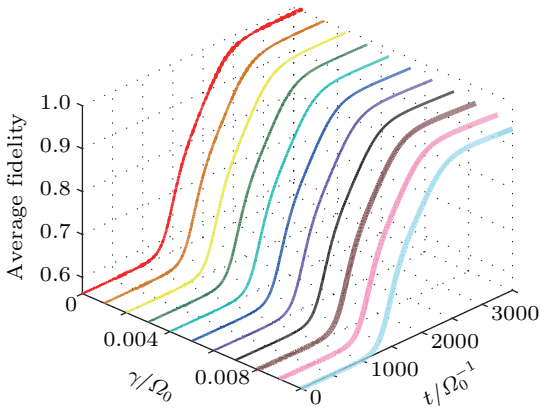


Fig. 6. (color online) Time-dependent variation of the average fidelity with different atomic total spontaneous emission rates. Parameters used here are the same as in Fig. 2.

5. Conclusion and prospect

We have accomplished the implementation of the two-qubit phase gate between two Rydberg atoms by combin-

ing adiabatic passage and Rydberg antiblockade. An effective single-photon detuning Λ-type three-level Hamiltonian is obtained in the Rydberg antiblockade regime, and a desired two-qubit π-phase gate is able to be executed by using the adiabatic-passage technique. The total Hamiltonian can give a relatively perfect result, which is pretty similar to that given by the effective Hamiltonian. Numerical simulations show that the fidelity with a specified initial state can always be over 95%. The average fidelity with actual experimental parameters is up to 98.7%, which proves that the proposed scheme for implementing the two-qubit phase gate is robust against atomic spontaneous emission.

In the past several years, a lot of methods or techniques, usually called "shortcuts to adiabatic passage" (STAP), have been proposed to speed up an adiabatic passage,[51–57] with which many schemes have proposed to achieve quantum information processing and quantum computation.[11,58–63] In addition, the combinations between RRI and STAP have been accomplished.[33,40,42] For prospects, therefore, the current scheme is supposed to be accelerated by STAP to construct a fast π-phase gate.

References

[1] Deutsch D 1985 *Proc. Roy. Soc. London Ser. A* **400** 97
[2] Grover L K 1997 *Phys. Rev. Lett.* **79** 325
[3] Grover L K 1998 *Phys. Rev. Lett.* **80** 4329
[4] DiVincenzo D P 1995 *Phys. Rev. A* **51** 1015
[5] Barenco A, Bennett C H, Cleve R, DiVincenzo D P, Margolus N, Shor P, Sleator T, Smolin J A and Weinfurter H 1995 *Phys. Rev. A* **52** 3457
[6] Jaksch D, Cirac J I, Zoller P, Rolston S L, Côté R and Lukin M D 2000 *Phys. Rev. Lett.* **85** 2208
[7] Yi X X, Su X H and You L 2003 *Phys. Rev. Lett.* **90** 097902
[8] Møller D, Madsen L B and Mølmer K 2008 *Phys. Rev. Lett.* **100** 170504
[9] Rao D D B and Mølmer K 2014 *Phys. Rev. A* **89** 030301(R)
[10] Liu X, Fang G Y, Liao Q H and Liu S T 2014 *Phys. Rev. A* **90** 062330
[11] Chen Y H, Xia Y, Chen Q Q and Song J 2015 *Phys. Rev. A* **91** 012325
[12] Borges H S and Villas-Bôas C J 2016 *Phys. Rev. A* **94** 052337
[13] Qin W, Wang X, Miranowicz A, Zhong Z and Nori F 2017 *Phys. Rev. A* **96** 012315
[14] Duan L M, Wang B and Kimble H J 2005 *Phys. Rev. A* **72** 032333
[15] Deng Z J, Zhang X L, Wei H, Gao K L and Feng M 2007 *Phys. Rev. A* **76** 044305
[16] Cirac J I and Zoller P 1995 *Phys. Rev. Lett.* **74** 4091
[17] Kang Y H, Xia Y and Lu P M 2016 *Quantum Inf. Process.* **15** 4521
[18] Shao X Q, Zhu A D, Zhang S, Chung J S and Yeon K H 2007 *Phys. Rev. A* **75** 034307
[19] Zhang Y Q and Zhang S 2009 *Chin. Phys. B* **18** 4683
[20] Zheng S B 2009 *Chin. Phys. B* **18** 3453
[21] Gershenfeld N A and Chuang I L 1997 *Science* **275** 350
[22] Yang C P and Han S 2006 *Phys. Rev. A* **73** 032317
[23] Shao X Q, Zhao Y F, Zhang S and Chen L 2009 *Chin. Phys. B* **18** 5161
[24] Saffman M, Walker T G and Mølmer K 2010 *Rev. Mod. Phys.* **82** 2313
[25] Jaksch D, Cirac J I, Zoller P, Rolston S L, R Côté and Lukin M D 2000 *Phys. Rev. Lett.* **85** 2208
[26] Lukin M D, Fleischhauer M, R Côté, Duan L M, Jaksch D, Cirac J I and Zoller P 2001 *Phys. Rev. Lett.* **87** 037901
[27] Shao X Q, Zheng T Y, Oh C H and Zhang S 2014 *J. Opt. Soc. Am. B* **31** 827
[28] Shao X Q, You J B, Zheng T Y, Oh C H and Zhang S 2014 *Phys. Rev. A* **89** 052313
[29] Su S L, Guo Q, Wang H F and Zhang S 2015 *Phys. Rev. A* **92** 022328
[30] Shao X Q, Wu J H and Yi X X 2017 *Phys. Rev. A* **95** 022317
[31] Shao X Q, Wu J H, Yi X X and Long G L 2017 *Phys. Rev. A* **96** 062315
[32] Zhao P Z, Cui X D, Xu G F, Sjöqvist E and Tong D M 2017 *Phys. Rev. A* **96** 052316
[33] Kang Y H, Chen Y H, Shi Z C, Huang B H, Song J and Xia Y 2018 *Phys. Rev. A* **97** 042336
[34] Yan D, Cui C L, Zhang M and Wu J H 2011 *Phys. Rev. A* **84** 043405
[35] Tian X D, Liu Y M, Cui C L and Wu J H 2015 *Phys. Rev. A* **92** 063411
[36] Su S L, Liang E, Zhang S, Wen J J, Sun L L, Jin Z and Zhu A D 2016 *Phys. Rev. A* **93** 012306
[37] Su S L, Gao Y, Liang E and Zhang S 2017 *Phys. Rev. A* **92** 022319
[38] Su S L, Tian Y, Shen H Z, Zang H, Liang E and Zhang S 2017 *Phys. Rev. A* **96** 042335
[39] Shao X Q, Wu J H and Yi X X 2017 *Phys. Rev. A* **95** 062339
[40] Shao X Q, Li D X, Ji Y Q, Wu J H and Yi X X 2017 *Phys. Rev. A* **96** 012328
[41] Ji Y Q, Dai C M, Shao X Q and Yi X X 2017 *Quantum Inf. Process.* **16** 259
[42] Zhao Y J, Liu B, Ji Y Q, Tang S Q and Shao X Q 2017 *Sci. Rep.* **7** 16489
[43] Chen Y H, Shi Z C, Song J, Xia Y and Zheng S B 2018 *Phys. Rev. A* **97** 032328
[44] James D F V and Jerke J 2007 *Can. J. Phys.* **85** 625
[45] Born M and Fock V 1928 *Zeitschrift für Physik* **51** 165
[46] Bergmann K, Theuer H and Shore B W 1998 *Rev. Mod. Phys.* **70** 1003
[47] Berry M V 1984 *Proc. R. Soc. A* **392** 45
[48] Chen Y H, Wu Q C, Huang B H, Song J and Xia Y 2016 *Sci. Rep.* **6** 38484
[49] Gaëtan A, Miroshnychenko Y, Wilk T, Chotia A, Viteau M, Comparat D, Pillet P, Browaeys A and Grangier P 2009 *Nat. Phys.* **5** 115
[50] Miroshnychenko Y, Gaëtan A, Evellin C, Grangier P, Comparat D, Pillet P, Wilk T and Browaeys A 2010 *Phys. Rev. A* **82** 013405
[51] Chen X, Lizuain I, Ruschhaupt A, Guéry-Odelin D and Muga J G 2010 *Phys. Rev. Lett.* **105** 123003
[52] del Campo A 2013 *Phys. Rev. Lett.* **111** 100502
[53] Ibáñez S, Chen X, Torrontegui E, Muga J G and Ruschhaupt A 2012 *Phys. Rev. Lett.* **109** 100403
[54] Song X K, Ai Q, Qiu J and Deng F G 2016 *Phys. Rev. A* **93** 052324
[55] Chen Y H, Xia Y, Wu Q C, Huang B H and Song J 2016 *Phys. Rev. A* **93** 052109
[56] Baksic A, Ribeiro H and Clerk A A 2016 *Phys. Rev. Lett.* **116** 230503
[57] Wu Q C, Chen Y H, Huang B H, Song J, Xia Y and Zheng S B 2016 *Opt. Express* **24** 22847
[58] Chen Y H, Xia Y, Chen Q Q and Song J 2014 *Phys. Rev. A* **89** 033856
[59] Chen Y H, Xia Y, Chen Q Q and Song J 2014 *Laser Phys. Lett.* **11** 115201
[60] Chen Y H, Xia Y, Song J and Chen Q Q 2015 *Sci. Rep.* **5** 15616
[61] Chen Z, Chen Y H, Song J, Xia Y and Huang B H 2016 *Sci. Rep.* **6** 22202
[62] Yu L, Xu J, Wu J L and Ji X 2017 *Chin. Phys. B* **26** 060306
[63] Xu J, Yu L, Wu J L and Ji X 2017 *Chin. Phys. B* **26** 090301